

Received: 13 November 2024 / Accepted: 04 October 2024 / Published online: 07 October 2024

*suspension, damping,  
shock absorber,  
dynamic characteristics*

Marek STEMBALSKI<sup>1\*</sup>  
Tomasz SZYDŁOWSKI<sup>2</sup>  
Arkadiusz CZARNUCH<sup>3</sup>

## **INFLUENCE OF SHOCK ABSORBER ON ELECTRIC AXLE VIBRATION IN SEMI-TRAILER**

This article describes the results of a study of the effect of a shock absorber on the vibration of an electric axle in a semi-trailer. The dynamic characteristics of three shock absorbers from different manufacturers were determined. They were then installed on the electric axle of a semi-trailer equipped with a measuring apparatus. Test runs were carried out on two types of road surface - a test track with a defined profile and a local road. Each run was repeated for a fully loaded and an empty semi-trailer. These tests were designed to determine the values of the dynamic parameters of the electric axle during operation of the semi-trailer depending on the shock absorber used.

### **1. INTRODUCTION**

Interest in electric and hybrid cars has increased in recent years. Taking the Polish market as an example, there has been a 70% increase in the registration of new all-electric passenger cars, an 86% increase in the registration of electric vans (over 3.5 t) and a 556% increase in the registration of electric trucks [1]. On the other hand, if one compares the European Union market (Fig. 1), electric or hybrid cars account for more than 48% of the market [2]. In the previous year, the ratio was at 51%.

Recent years of automotive development have seen a constant drive to reduce the negative impact of vehicle use on the environment. The development efforts undertaken apply not only to passenger cars, but also to heavy vehicles.

As required by European authorities, all EU countries must link truck tolls to CO<sub>2</sub> emissions. The principle is simple - the more CO<sub>2</sub> you emit, the more you have to pay. A key tool for calculating CO<sub>2</sub> emissions for a specific model and configuration is VECTO (Vehicle Energy Consumption Calculation Tool). The VECTO score actually determines how economical a vehicle is.

---

<sup>1</sup> Faculty of Mechanical Engineering, Department of Machine Tools and Mechanical Technologies, Wrocław University of Science and Technology, Poland

<sup>2</sup> Department of Vehicles and Fundamentals of Machine Design, Lodz University of Technology, Poland

<sup>3</sup> Wielton S.A., 98-300 Wielun, Poland

\* E-mail: marek.stembalski@pwr.edu.pl

<https://doi.org/10.36897/jme/194150>

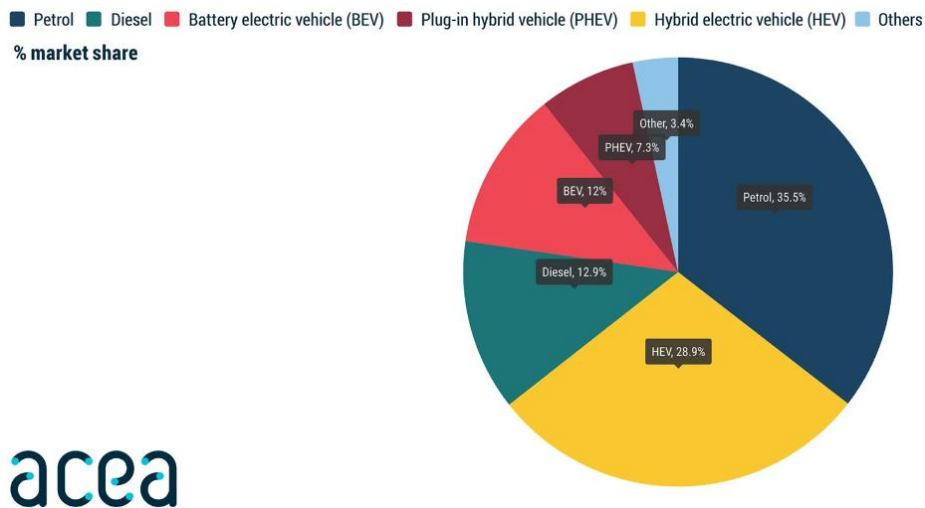


Fig. 1. New EU cars by power source, February 2024 [2]

European Commission regulations stipulate that even manufacturers will be forced to significantly reduce CO<sub>2</sub> emissions by 2030 even from trailers. VECTO was developed by the European Commission to use a series of parameters to calculate a truck's fuel consumption and thus carbon dioxide emissions. This sends a clear signal to the industry to accelerate the market introduction of energy-efficient technologies and zero- and low-emission heavy vehicles. Current solutions used by trailer manufacturers to reduce fuel consumption and thus reduce CO<sub>2</sub> emissions are aerodynamic kits that reduce drag by up to 26% [3]. Even a simple side cover reduces drag by up to 14%, resulting in a 7% reduction in fuel consumption [4]. In addition, photovoltaic systems are being introduced on fixed-roof trailers to generate additional electricity.

Another step to reduce the energy intensity of articulated vehicles, as well as improving their traction characteristics, is the use of electric axles in trailers. Preliminary studies show that they will reduce fuel consumption by up to 25%. Such axles will be able to recover energy in the braking process. In addition, an extremely important advantage of such solutions will be the possibility to use the drive of a semi-trailer in difficult road conditions, such as when driving up a hill - improving traction properties - or when starting off, when it will significantly reduce the load on the combustion engine. Many manufacturers already offer such solutions. For example the French company Adgero's solution, UltraBoost, allows energy to be recovered during braking and stored in small ultracapacitors with significant capacity. The recuperated mechanical energy converted into electricity can also be used to drive a refrigeration unit, such as in the case of SAF Holland's solution called TRAKr [5]. The above-mentioned company also has a solution called TRAKe, which is a semi-trailer axle with an additional electric drive to drive the wheels of the semi-trailer. The tangible effects of such a solution are the relief of the internal combustion engine of the semi-trailer tractor, thus reducing fuel consumption and improving the dynamics of the vehicle combination, as well as significant advantages for the traction of such a vehicle combination. Company representatives also emphasise that the presented solution has the additional advantage of being able to reduce vehicle noise, which meets the challenges of delivering goods to cities at night.

An electric axle solution was also presented by BOSCH . The concept envisages that the electrical energy recovered during braking will be stored in batteries and the control system will use it as required, e.g. to: drive a refrigeration unit, to support the drive of a tractor-trailer, to self-propel trailers allowing the trailer to move by itself (possible, for example, using a remote control system).

Developed by BPW, the ePower solution [6] is an axle module that recovers energy while the trailer is moving, enabling a carbon-neutral and quiet energy supply to refrigeration units for temperature-controlled transport.

The possibilities of using electric axles in trailers have also been recognised and offered by companies such as Schmitz, Krone, ZF//WABCO, TrailerDynamics and Wielton.

In publications [7, 8], the authors presented the results of theoretical and field tests of agricultural tractors with trailers, indicating the advantages of using trailer axle drive of an articulated vehicle. The use of electric axles in semi-trailers makes it necessary to take into account the effect of increased unsprung masses in the suspension operation.

Electric axles are widely used in the automotive industry. A publication [9] compared the life cycle of an integrated electric axle with powertrains for electric and conventional passenger cars. Gennaro et al [10] described how to design an integrated electric axle for third-generation electric vehicles.

Based on data from leasing companies (e.g.: DKV, EUROWAG), ACEA reports, telematics analyses and studies (e.g.: Geotab, TomTom Telematics) and European Commission reports, it can be assumed that the average annual mileage of trucks is around 100,000 km. Assuming a savings of 10% with an electric axle, the annual savings from this can reach about €4,500 per vehicle. The calculation assumes an average fuel consumption of 30 liters per 100 km. Greater savings can be achieved with an increase in driving dynamics. Then the fuel consumption can go as high as 60 liters per 100 km, and the savings from the use of an electric axle can exceed 20%.

Suspension components with a significant impact on safety are shock absorbers. An efficient suspension shock absorber, properly selected for the vehicle, ensures both passenger and driver comfort [11] and driving safety. The shock absorber is also responsible for wheel contact with the ground. In addition, the shock absorber can, through its design, contribute to reducing energy consumption during driving [12].

An in-depth review of regenerative shock absorber solutions was developed by Tiwarii et al [13]. Another solution for a shock absorber that stores energy while driving in a large bus-type vehicle was presented by Ali A. and others [14] using, among other things, a cam mechanism. Galuzzi R. et al [15], on the other hand, proposed a compact solution of a rotating generatrix shock absorber allowing energy recovery from road irregularities. The fabricated prototype was tested for damping capacity, total conversion efficiency and acoustic behaviour. Rotary dampers of this type would have applications in the automotive industry. Simulation considerations for the use of rotary shock absorbers in a passenger car were described by Tae Dong et al [16].

As far as commercial trailers are concerned, the state of wear of shock absorbers is not inspected during technical inspections. Only a visual assessment of the shock absorbers is performed. A shock absorber that is no longer serviceable is deemed to be leaking. Such a shock absorber should be replaced immediately. In the article [17], the authors carried out

tests to check the effect of vertical shock absorber loads transferred to the road surface, taking into account the condition of shock absorbers in the front suspension of a truck.

Shock absorber tests are widely reported in the literature, e.g. Li [18] conducted a study of magnetic shock absorbers used in aviation. Lukczo [19] presented a numerical analysis of a quarter car using a hydraulic shock absorber. Guan [20], on the other hand, described experimental and simulation studies for a two-tube hydraulic shock absorber. On the other hand, in [21], the authors conducted an analysis of the dynamic properties and operational safety of railroad cars using rubber-metal shock absorbers between the disc elements of railroad cars. Also [22], the authors presented a study of a regenerative shock absorber with damping capability used in freight cars.

The authors of this article focused on the measurements of the new shock absorbers by determining their dynamic characteristics and carried out road tests involving runs on a test track with a defined road profile and runs on a local road. On this basis, the effect of the shock absorber on the vibration of the electric axle was determined. The result of the research described in the article should be an answer to the question of whether the use of shock absorbers from different manufacturers will affect the operating conditions of the electric axle and what maximum values of parameters such as acceleration and displacement will be achieved during test runs of the semi-trailer with an electric axle.

## 2. METHODOLOGY OF RESEARCH

The first stage of the research was to determine the dynamic characteristics of the new shock absorbers. The shock absorbers tested were mounted as part of a semi-trailer suspension with an electric axle. The shock absorbers from different manufacturers, designated for the purpose of this article as shock absorber 1, shock absorber 2 and shock absorber 3, were tested. The maximum values of the forces during tension and compression of the shock absorbers were then compared as a function of their mileage. The second stage of the study was to check the damping of each shock absorber when tested on a test track and one of the shock absorbers on an inferior local road. A detailed description of the test conditions (including semi-trailer loading) is described in subsection 2.2.2 of the article. Figure 2 shows a schematic of the procedure for the tests carried out.

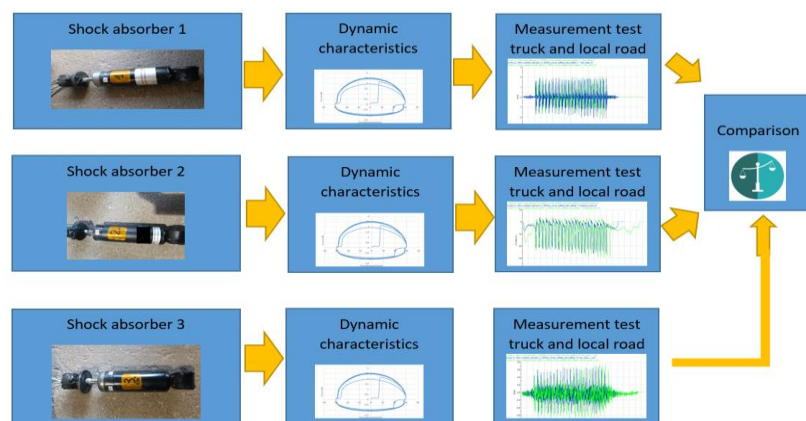


Fig. 2. Diagram of the tests carried out

## 2.1. OBJECT OF RESEARCH

Shock absorbers designed for the air suspension of a 3-axle semi-trailer were used for the tests. The axle load capacity of the semi-trailers tested is 9 t. Two shock absorbers are mounted on the axle of the semi-trailer. The upper part of the shock absorber is supported by the main bracket of the half-spring, the lower part is attached to the axle behind the half-spring (Fig. 3.). Due to the possibility of damage during testing to the electronic systems or electric motors, it was decided to mount weights in the lower part of the axle to imitate the weight of these systems together with the electric motors.

Shock absorbers with a stroke of 160 mm were used during the tests. Before testing, the piston rod covers of each shock absorber were cut. In addition, in order to achieve greater deformation of the shock absorber piston rod and thus greater sensitivity of the strain gauge measuring system, a technological undercut was made on the shock absorber piston rod. An undercut of 0.5 mm per side was then made on their piston rods (Fig. 4A). On the surface of the undercut, four strain gauge rosettes spaced around the circumference of the piston rod were glued on and connected in a system of 4 Wheatstone half-bridges (Fig. 4B). In the remainder of this article, the measurement results from the individual strain gauge bridges are labelled T1–T4.

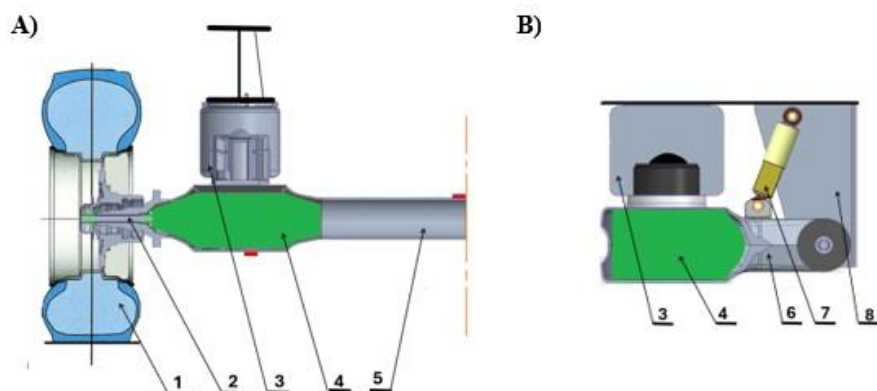


Fig. 3. Scheme of the electrical axis. A) cross-section B) longitudinal section. 1) wheel, 2) transmission shaft, 3) suspension cushion, 4) electric motor system space, 5) axle, 6) half-spring, 7) shock absorber, 8) suspension bracket

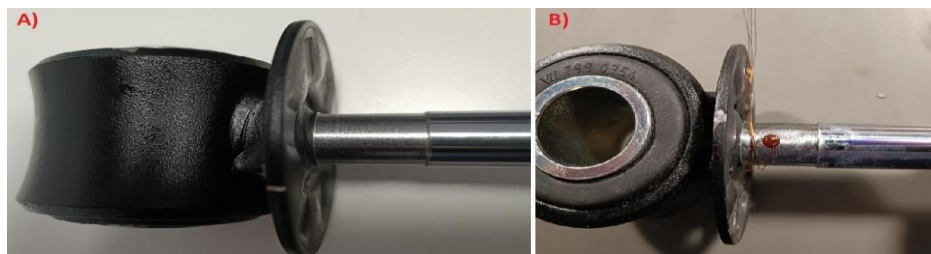


Fig. 4. Preparation of shock absorbers for testing

In addition, using customised clamps, cable sensors were mounted on each shock absorber to measure the amplitude of displacement of the shock absorber itself during testing on the test track (Fig. 5).

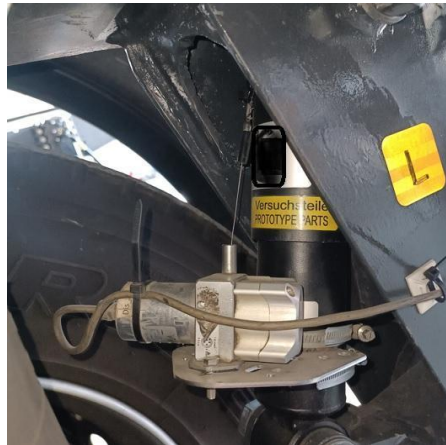


Fig. 5. Shock absorber with cable displacement sensor fitted to the trailer suspension system

## 2.2. MEASURING TECHNIQUE

### 2.2.1. THE DURABILITY MACHINE

As part of the study, the dynamic characteristics of the shock absorbers were determined in tension and compression. For this purpose, a single-axis Instron durability test machine model 8872 [23] was used, which has an operating range of up to  $\pm 25$  kN with a useful stroke of up to 100 mm. The shock absorber under test was mounted in the jaws of the machine using designed adapters. The recording of parameters (force and displacement over time) was carried out using a computer with appropriate software supplied by Instron. The sampling frequency of the recorded signals was 50 Hz. A view of the entire measuring station is shown in Fig. 5.

The measurement cycle was as follows. During the test, cyclic sinusoidal excitations were set at variable frequencies, from 0.1 to 1.1 Hz, with steps of 0.2 Hz. The time course of the cyclic forcing on the durability machine is shown in Fig. 6.

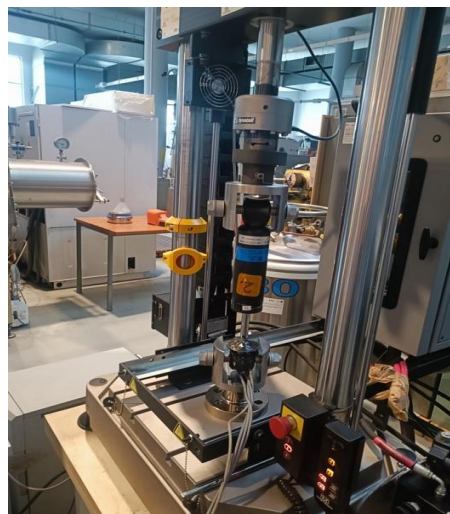


Fig. 6. View of the shock absorber mounted on the durability machine

For each frequency, the velocity and force for the compression and tension cycles of the individual dampers were determined. The amplitude of the forcing was in the range  $\pm 30$  mm.

### 2.2.2. ROAD TESTS

During the tests on the test track, the first axle of the semi-trailer was fitted with 19 sensors to record various physical values in real time, including the acceleration of the axle, the pressure in the axle's pneumatic system, the tension on the shock absorber piston rod, as well as the displacement between the axle and the displacement of the shock absorber piston rod. In most cases the electric axle on semi-trailers is mounted as the middle axle. Prior to the tests, it was decided to mount the electric axle as the first axle because the semi-trailer was to be subjected to additional tests, including the violent forcing involving driving over a curb. This part of the tests will be the subject of a future publication.

Details of the individual sensors used during the tests are presented below, and Fig. 7 shows schematically the locations of the measuring sensors, while Tables 1,2,3 show the location of the sensors on the real object.

- 1 MEMS capacitive accelerometer, measuring range  $\pm 300$  m/s<sup>2</sup> with measurement in two axes (3 channels), frequency response ( $\pm 3$  dB) 0 to 4000: located in the centre of the axes measuring transverse and longitudinal accelerations in the direction of travel,
- 7 MEMS capacitive accelerometers, measuring range  $\pm 300$  m/s<sup>2</sup> with measurement in one vertical axis frequency response ( $\pm 3$  dB) 0 to 4000: located on the lower chassis near the suspension cushion, on the suspension supports, near the wheels and in the lower part of the axle (where weights imitating an electric motor are attached 66 kg per axle),
- 4 displacement sensors, measuring range  $\pm 0.32$  m with a linearity of  $\pm 0.02\%$ , mounted on the shock absorber to measure piston rod displacement and on the lower chassis to measure the relative displacement between the axle and the frame of the semi-trailer,
- 4 half-bridge strain gauges 120  $\Omega$ , one strain gauge active and one passive: mounted on the piston rod of the shock absorber,
- 2 pressure sensors, measuring range 0–200 MPa, rated sensitivity  $2 \pm 2\%$  mV/V: in every airbag of the suspension.

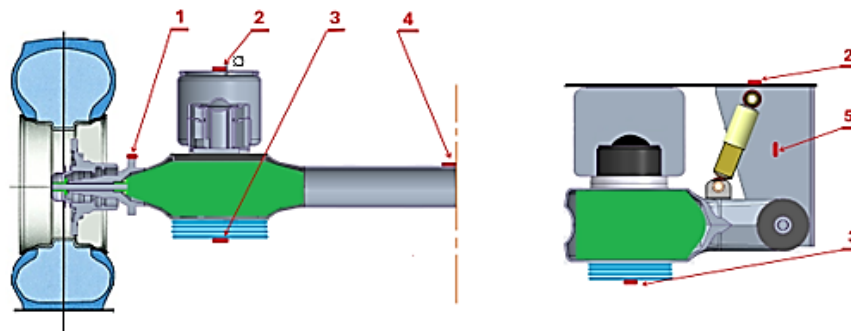


Fig. 7. Distribution of accelerometers on the axle and suspension 1 - on the axle near the wheel, 2- on the vehicle frame, 3 - under the axle where the electric motor is attached 4 - on the centre of the axle 5 - on the suspension bracket

Quantum HBM series measurement cards were used for data acquisition. The data were recorded with a CX22 data recorder. The measurement frequency for each channel amounted to 300 Hz. A 50 Hz low-pass filter was used during data recording.

Table 1. Position of strain gauges

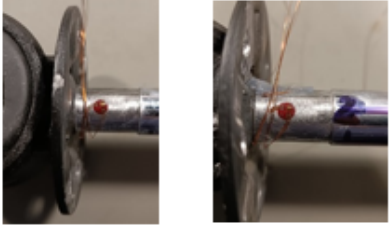






<b>1</b>	<i>Sensor type</i>	<b>Strain gauge</b>	<i>Measurement card:</i>	
No.	Number	Position	Type	Pictures
1	R1, R2, R3, R4 (X,Y,Z)	The strain gauges are placed on the piston rod near the shock absorber head. Strain gauge rosettes spaced 90 degrees.	Tens k - 2,16	

Table 2. Position of acceleration

<i>Sensor type</i>		<b>Accelerometer</b>	<i>Location</i>	
No	Name	Position	Type	Pictures
1	ACC_Brack_R	Right side Bracket	ACC	
2	ACC_Brack_L	Left side Bracket	ACC	
3	ACC_Axle_down_L	down on the axle - left side	ACC	
4	ACC_Flange_L	lower belt left side	ACC	
5	ACC_Flange_R	lower belt right side	ACC	
6	ACC_Axle_down_L	down on the axle - left side	ACC	
7	ACC_Axle_L_vert	Axle left side	ACC	
8	ACC_Axle_middle_X	Middle axle	ACC	
9	ACC_Axle_middle_Y			



Table 3. Position of pressure and displacement sensors

Sensor type		Displacement sensor	Measurement card: MX840B	
No	Number	Position	Type	Pictures
1	Pressure_1R	1 axis right side	Pressure	
2	Pressure_1L	1 axis left side	Pressure	
3	Distance_Axle_R	Position on the lower belt behind 1 axis on the right, control of the change in the distance between the axis and the lower belt.	DIS	
4	Distance_Axle_L	Position on the lower belt behind 1 axis on the left, control of the change in the distance between the axis and the lower belt.	DIS	
5	Distance_Am_R	Position on the shock absorber, on the right side, control displacement the piston	DIS	
6	Distance_AM_L	Position on the shock absorber, on the left side, control displacement the piston	DIS	

The tests were carried out for two configurations. In the first step, a test track was used, while in the second step, data was collected from a local road of poorer quality. The tests on the test track consisted of driving through one selected road profile of the sleeping policeman type. The drive was carried out at a speed of 15 km/h. The semi-trailer was loaded with a uniform load of 24 t. There were 25 obstacles of this type distributed over a distance of several tens of metres. They the same height. A view of a section of the test track is shown in Fig. 8. As far as the local road is concerned, measured data was collected while driving through a 20-kilometre section of a local road that is visually inferior to national roads or motorways. This was done with a loaded and unloaded semi-trailer in which shock absorber No. 1 was fitted.



Fig. 8. View of a section of the test track

### 3. TEST RESULTS

#### 3.1. CHARACTERISTICS OF SHOCK ABSORBERS

The first stage of the study was to check the maximum force values during the tension and compression of the shock absorber at different speeds. Fig. 9 shows a comparison of the dynamic characteristics for the three tested shock absorbers.

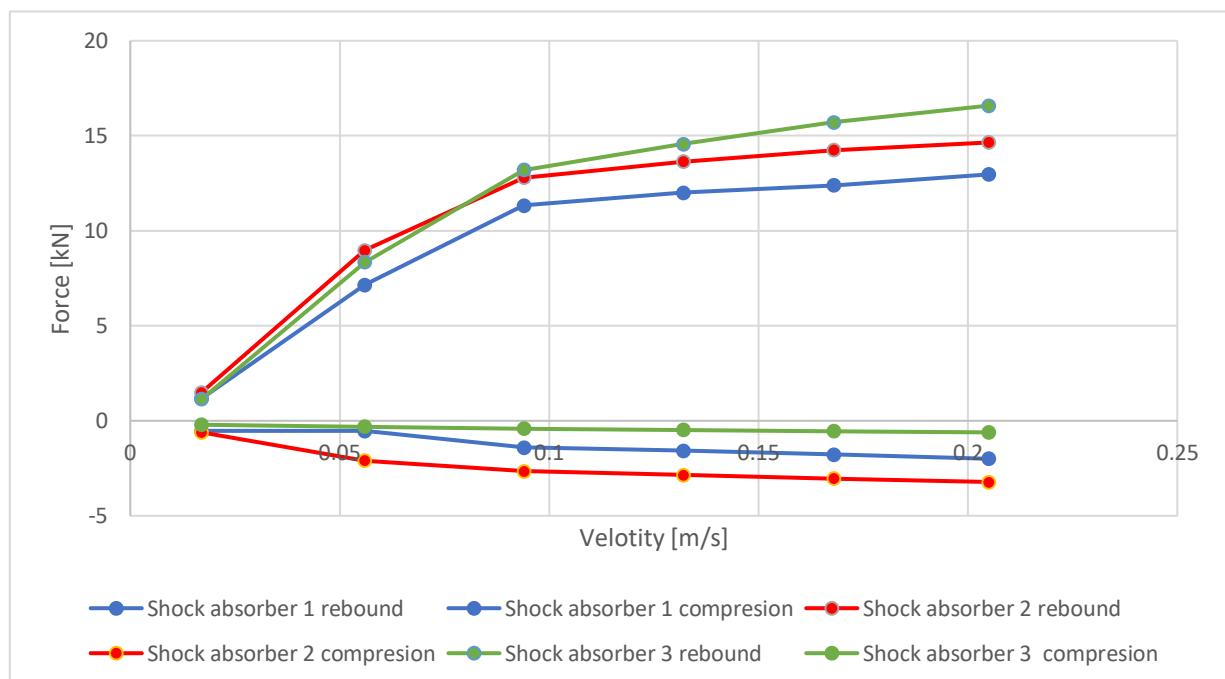


Fig. 9. Damping force characteristics of shock absorbers

Analysing the results obtained, it should be noted that the maximum tensile values were obtained on shock absorber No. 3. The values were 28% higher than for shock absorber No. 1, which had the lowest tensile value. The difference between shock absorber No. 1 and 2 was 13%, and between shock absorber No. 2 and 3 15%.

### 3.2. ROAD TESTS RESULTS

Mainly data from displacement sensors and accelerometers were taken into account to analyse the results. In the figures below, “range” (pik to pik amplitude) indicates the measurement range, which was calculated from the difference between the positive and negative maximum amplitude values. The stresses measured on the piston rods of the dampers measured during the tests varied from 100–150 MPa.

The results of measuring displacement and acceleration when passing over the road profile on the test track are shown in Fig. 10–11, while Fig. 12–13 shows the difference in measured displacement and acceleration depending on the load on the semi-trailer.

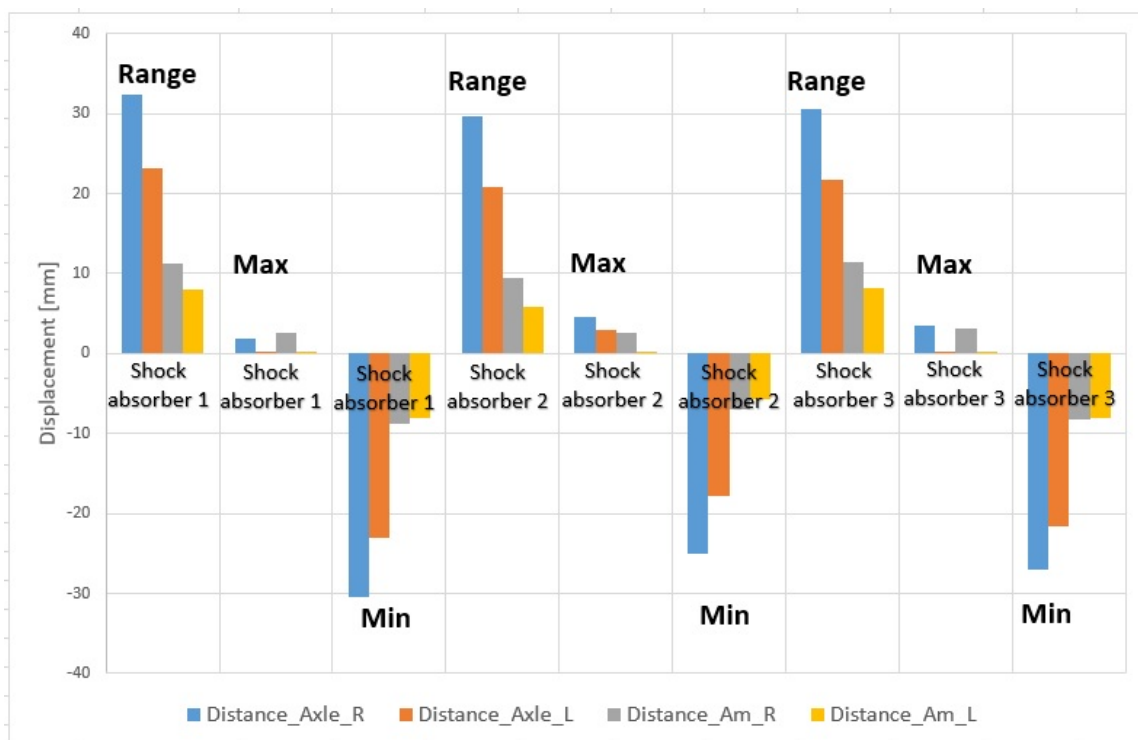


Fig. 10. Comparison of the amplitude of displacement of the axle and the piston rod of the shock absorbers during driving through the test track

When analysing the displacement ranges for individual shock absorbers, it should be noted that both in the case of the relative axle displacement and the piston rod displacement amplitude, the smallest amplitudes were recorded for shock absorber no. 2. On the other hand, the largest amplitudes were recorded for shock absorber No. 1. The difference between shock absorber no. 1 and 2 was up to 40%. However, the difference in measured amplitude between shock absorber No. 1 and 3 was a maximum of 7%.

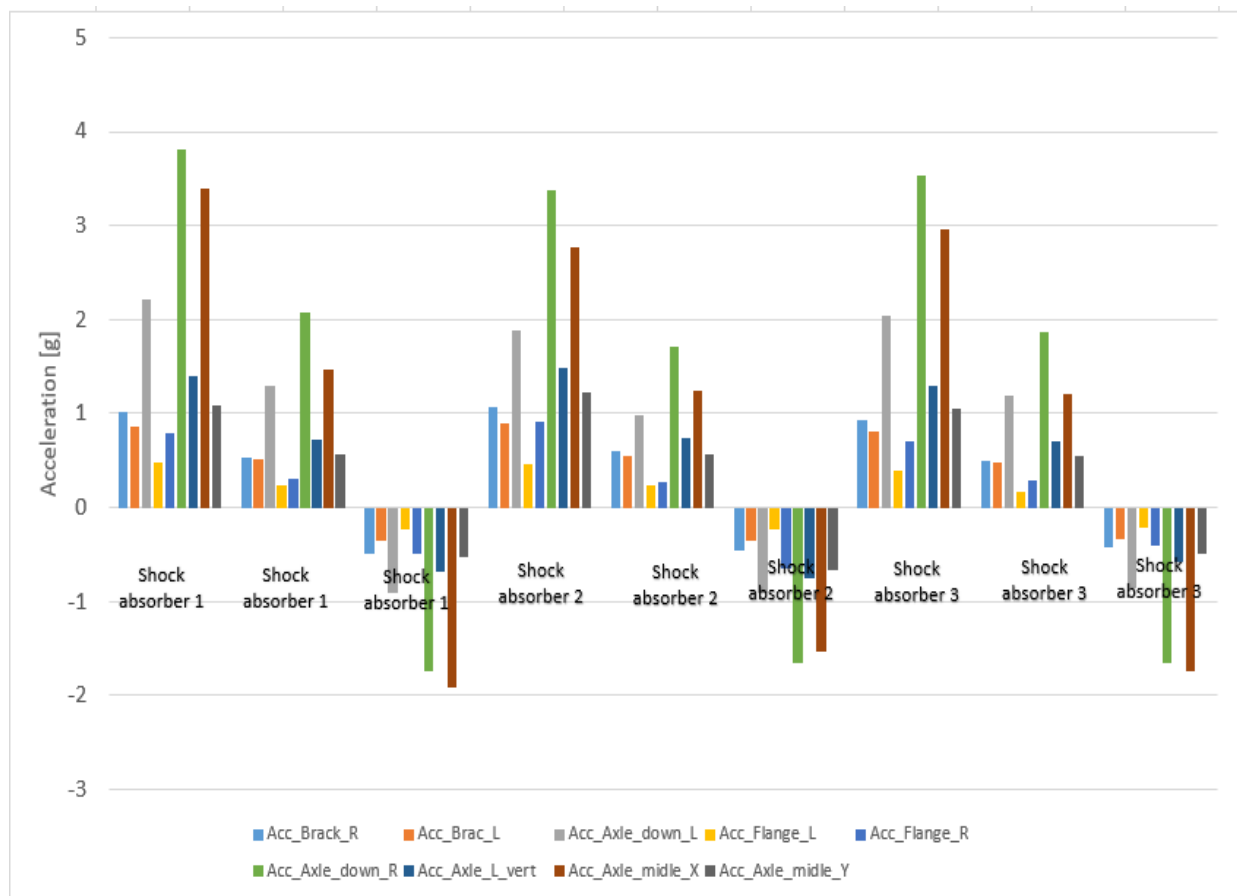


Fig. 11. Comparison of the amplitude of acceleration when passing through the test track

Analysing the ranges of measured accelerations, it should be noted that analogous results were obtained to those for displacement. The highest accelerations were measured in the suspension in which shock absorber No. 1 was fitted, while the lowest acceleration values were recorded at shock absorber No. 2.

On the other hand, if we look at the acceleration values measured on the trailer frame in relation to the signal on the axle, it turns out that the suspension in which shock absorber No. 3 was fitted has the highest damping value. The accelerometers were located according to the Table 2: accelerometers numbered 1, 2, 4, 5 were located on the axle bracket and the semi-trailer lower belt, respectively; accelerometers numbered 3, 6-9 were located on the axle.

Comparing the range of displacement amplitudes (the difference between the maximum and minimum amplitudes), it can be seen that in all cases the value of the axle displacement for the vehicle with 24 t load is greater than for the unladen vehicle. The relative displacement between the semi-trailer axle and the semi-trailer frame is 10% greater for the laden semi-trailer. On the other hand, the displacement of the piston rod of the shock absorber is 38% greater for a loaded semi-trailer than for an unloaded vehicle.

Comparing the range of acceleration amplitudes (the difference between the maximum and minimum amplitudes), it can be seen that, in all cases, the axle acceleration value for a vehicle loaded with 24 t is greater than for an unloaded vehicle. The percentage differences range from 2% to 68%, depending on the measurement location selected.

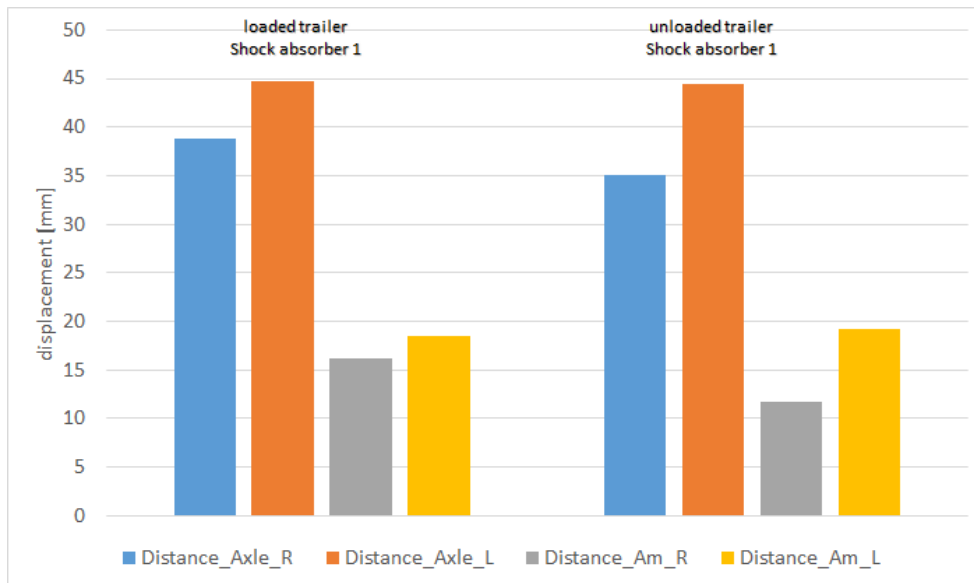


Fig. 12. Comparison of axle-to-frame displacement for loaded and unloaded semi-trailer

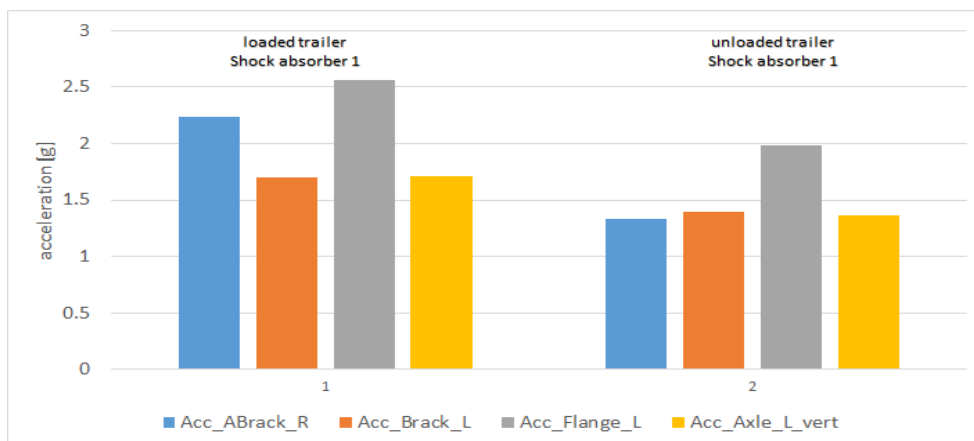


Fig. 13. Comparison of acceleration at selected suspension points for loaded and unloaded semi-trailer - range of acceleration amplitude measured

#### 4. CONCLUSION

Analysis of the test results shows a clear effect of the load on the amplitudes of the suspension displacement and acceleration of the axle as well as the trailer frame. The recorded accelerations of the axle loaded with electric motors were in the range up to 4g. This type of information should be taken into account by designers when designing the motors used in electric axles.

This paper presents the initial stage of the work that will be carried out to develop a reliable semi-trailer drive. It made possible to identify and solve problems related to the test methodology, measurement apparatus and methods of analysing the data obtained. The results also provide valuable material for future research into the dynamic properties of the semi-trailers with electric axles.

## REFERENCES

- [1] [https://psnm.org/wpcontent/uploads/2024/01/PSPA\\_Rok\\_2023\\_w\\_polskiej\\_elektromobilnosci\\_Raport.pdf](https://psnm.org/wpcontent/uploads/2024/01/PSPA_Rok_2023_w_polskiej_elektromobilnosci_Raport.pdf).
- [2] <https://elektromobilni.pl/samochody-elektryczne-na-stabilnym-poziomie-w-ue/>.
- [3] CHOWDHURY H., MORIA H., ALI A., KHAN I., 2013, *A Study on Aerodynamic Drag of a Semi-Trailer Truck*, *Procedia Engineering*, 56, 201–205.
- [4] VAN RAEMDONCK G., VON TOOREN M., 2008, *Design of an Aerodynamic Aid for the Underbody of a Trailer Within a Tractor-Trailer Combination*, *BBA VI International Colloquium on Bluff Bodies Aerodynamic & Application*, 20–24.
- [5] [https://safholland.com/mide/en/downloadcenter/document/resource/environment/project1\\_p/documents/documentationP/2022/2022\\_09/SAF-HOLLAND\\_E-Axles\\_en-DE.pdf](https://safholland.com/mide/en/downloadcenter/document/resource/environment/project1_p/documents/documentationP/2022/2022_09/SAF-HOLLAND_E-Axles_en-DE.pdf).
- [6] <https://www.bpw.de/en/products/axle-running-gears/epower>.
- [7] ZEMANEK T., PROCHAZKA P., PAZDERA I., NERUDA J., MERGL V., VITEK O., ULRICH R., STANEK L., 2022, *Operating Characteristics of a Timber Trailer with a Hybrid Drive*, *Forests*, 13/8, 1317, <https://doi.org/10.3390/f13081317>.
- [8] JANULEVICIUS A., PUPINIS G., 2013, *Power Circulation in Driveline System when the Wheels of Tractor and Trailer are Driven*, *Transport*, 28/3, 313–321, <https://doi.org/10.3846/16484142.2013.832378>.
- [9] KOROMA M.S., COSTA D., PURICELLI S., MESSAGIE M., 2023, *Life Cycle Assessment of a Novel Functionally Integrated E-Axle Compared with Powertrains for Electric and Conventional Passenger Cars*, *Science of the Total Environment*, 904, 166860.
- [10] DE GENNAROA M., PAGEA J.H., WELLERDIECKB T., et al., 2023, *Designing, Prototyping, and Testing an Integrated E-Axle for Third-Generation Electric Vehicles*, *Transportation Research Procedia*, 72, 101–108.
- [11] CALVO J.A., LOPEZ-BOADA B., ROMAN J.L.S., GAUCHIA A., 2009, *Influence of a Shock Absorber Model on Vehicle Dynamic Simulation*, *Proc. Inst. Mech. Eng. D: J. Automob. Eng.*, 223/2, 189–203, <https://doi.org/10.1243/09544070jauto990>.
- [12] MIRAGLIA M., TANNOUS M., INGLESE F., BRAMER B., MILAZZO M., STEFANINI C., 2022, *Energy Recovery from Shock Absorbers Through a Novel Compact Electro-Hydraulic System Architecture*, *Mechatronics*, 81, 102701.
- [13] TIWARI S., SINGH M., KUMAR A., 2020, *Regenerative Shock Absorber: Research Review*, *International Journal of Engineering Research & Technology (IJERT)*, 9/5.
- [14] ALI A., QI L., ZHANG T., LI H., AZAM A., ZHANG Z., 2021, *Design of Novel Energy-Harvesting Regenerative Shock Absorber Using Barrel Cam Follower Mechanism to Power the Auxiliaries of a Driverless Electric Bus*, *Sustainable Energy Technologies and Assessments*, 48, 101565, <https://doi.org/10.1016/j.seta.2021.101565>.
- [15] GALLUZZI R., CIRCOSTA S., AMATI N., TONOLI A., 2021, *Rotary Regenerative Shock Absorbers for Automotive Suspensions*, *Mechatronics*, 77, 102580, <https://doi.org/10.1016/j.mechatronics.2021.102580>.
- [16] TAE DONG K., JIN HO K., 2020, *Shock-Absorber Rotary Generator for Automotive Vibration Energy Harvesting*, *Appl. Sci.* 10/18, 6599, <https://doi.org/10.3390/app10186599>.
- [17] KUBO P., PAIVA C., FERREIRA A., LAROCCA A., 2015, *Influence of Shock Absorber Condition on Pavement Fatigue Using Relative Damage Concept*, *Journal of Traffic and Transportation Engineering*, 2/6, 406–413.
- [18] LI Y., LI D., 2021, *The Dynamics Analysis of a Magnetic Fluid Shock Absorber with Different Inner Surface Materials*, *Journal of Magnetism and Magnetic Materials*, 542, 168473, <https://doi.org/10.1016/j.jmmm.2021.168473>.
- [19] LUCZKO J., FERDEK U., 2019, *Non-Linear Analysis of a Quarter-Car Model with Strokedependent Twin-Tube Shock Absorber*, *Mechanical Systems and Signal Processing*, 115, 450–468, <https://doi.org/10.1016/j.ymssp.2018.06.008>.
- [20] GUAN D., JING X., SHEN H., JING L., GONG J., 2019, *Test and Simulation the Failure Characteristics of Twin Tube Shock Absorber*, *Mechanical Systems and Signal Processing*, 122, 707–719.
- [21] KARASSAYEVA A., ADILKHANOV Y., SEKEROVA S., JAPAYEV S., ZHAUYT A., ZHUNISBEK S., TERGEMES K., 2021, *Analysis of Dynamic Properties and Movement Safety of Bogies with Diagonal Links and Rubber-Metal Vibration Absorbers Between the Rubbing Elements of Freight Cars*, *Journal of Machine Engineering*, 2021, 21/3, 124–143.
- [22] DONG L., YANG F., HE A., GUO Z., YU J., ZUO J., 2022, *Investigation on Energy-Regenerative Shock Absorber with Adjustable Damping and Power for Freight Wagons*, *Energy Conversion and Management*, 254, 115228.
- [23] <https://www.instron.com/en/products/testing-systems/dynamic-and-fatigue-systems/servo-hydraulic-fatigue/8872-8874>.